Journal of the Franklin Institute 361 (2024) 1268–1283

Contents lists available at ScienceDirect

Journal of the Franklin Institute

journal homepage: www.elsevier.com/locate/fi

Dynamic event-triggered asynchronous filtering of Markovian jump systems against cyber-attacks

Chunlian Wang [a], Fangzheng Xue [a,*], Xiaojie Su [a], Xiaoyu Ma [b,c], Wengang Ao [d], Luis Ismael Minchala [e]

[a] School of Automation, Chongqing University, Chongqing, 400044, China
[b] Chengdu Research Institute, Sichuan University of Arts and Science, 635000, China
[c] Chongqing Co-core Intelligent Technology Research Institute Co. Ltd., 400021, China
[d] National Research Base of Intelligent Manufacturing Service, Chongqing Technology and Business University, No. 19, Xuefu Avenue, Nan'an District, Chongqing 400067, China
[e] Department of Electrical Engineering, Electronics and Telecommunications, University of Cuenca, Ave. 12 de Abril y Agustin Cueva, Cuenca 0101168, Ecuador

ARTICLE INFO

Keywords:
$\mathcal{H}_\infty$ asynchronous filtering
Markovian jump systems
Hidden Markovian model
Dynamic event-triggered

ABSTRACT

The paper focuses on the asynchronous filter design based on hidden Markovian model for Markovian jump systems with time-delay and external disturbances. Cyber nonlinearities in the communication environment are also considered. To further reduce the network bandwidth usage, an internal dynamic variable is introduced based on the previously extensively studied (static) event-triggered method, which is called dynamic event-triggered approach. The hidden Markovian model is utilized to characterize the asynchronous phenomenon caused by clock signals out of sync between system and filter mode. Then, according to the augmented filtering error system dynamics, some less conservative sufficient conditions are proposed to guarantee the stochastic stability with $\mathcal{H}_\infty$ performance. Consecutively, the filter parameter-solving problem is synthesized by a convex optimization problem. Finally, two numerical simulations are presented to demonstrate the effectiveness of the proposed approach.

1. Introduction

Practical physical applications always suffer from structural abrupt changes causing by random failures or component repairs, sudden environmental disturbances, and changing subsystem interconnections in the communication environment. Markovian jump systems (MJSs) are used for modeling this special type of stochastic system with these variations [1–4]. MJSs are quite popular among scholars—filter design [5,6], dissipative control [7,8] and sliding mode controller design [9,10] in many industries such as circuit systems [11] and multi-agent systems [12]. Through the communication link, there exist inevitable uncertainties and disturbances such as cyber-attacks [13,14]. A cyber attack refers to any type of attack on a computer information system, infrastructure, computer network or personal computer equipment [15]. With respect to computers and computer networks, unauthorized destruction, exposure, modification, disabling of software or services, theft or access to any computer data will be considered an attack on computers and computer networks [16–18]. The cyber nonlinearities usually result from the harsh environments such as uncontrollable elements (e.g., Network signal, Network dropouts, etc.) and aggressive conditions. In real-world

* Corresponding author.
E-mail addresses: wangchunlian@cqu.edu.cn (C. Wang), xuefangzheng@cqu.edu.cn (F. Xue), suxiaojie@cqu.edu.cn (X. Su), 20200095@sasu.edu.cn (X. Ma), aowg@ctbu.edu.cn (W. Ao), ismael.minchala@ucuenca.edu.ec (L.I. Minchala).

https://doi.org/10.1016/j.jfranklin.2023.12.007
Received 30 May 2023; Received in revised form 2 October 2023; Accepted 5 December 2023
Available online 29 December 2023
0016-0032/

applications, nonlinearity is inevitable for cyber-attacks, resulting in filtering problems for suppressing and preventing disturbances. In practical communication link applications, the cyber nonlinearities may occur in a probabilistic way [13]. Since the cyber nonlinearity cannot be simply ignored and often lead to poor performance of the controlled system, it is meaningful to solve the filtering problems for MJSs with nonlinear cyber-attack and this is one motivation of our work.

Filtering is a fairly important step in signal processing on disturbances [19] and noises [20], which can seriously affect the performance of the system. As is well known, filter problems exist widely in various practical applications including electronic technology [21], power electronics [22], aerospace science [23], signal/image processing [24,25]. Generally, filter design is divided into two parts: mode-dependent and mode-independent. When it comes to mode-dependent filters, as the name implies, the filter mode depends on the Markov chain state of the underlying system, and is usually supposed to be that the filter can be accessed at any time. This assumption is a little ideal, especially for the MJSs without time information. For example, in [26], the mode-dependent filter was designed firstly under the assumption of the measurable Markovian parameter. This inevitably limits the application of the mode-dependent filters, which prompts the development of mode-independent filters. It is quite effective when the system states are completely inaccessible. Similarly in [26], the mode-independent filter was designed without the assumption. Instead, note that mode-independent filters cannot handle the complicated asynchrony between the system mode and the filter mode, because they ignore all available mode information, which inevitably causes conservatism to a certain extent [27]. Therefore, it is necessary for us to design a novel hidden Markov model-based asynchronous filter, which is another motivation of our work.

In practical communication link, the network bandwidth is not limitless. Thus event-triggered method is arose to reduce the network bandwidth usage and save the network resource. There are a lot of scholars working on this and have produced many meaningful articles [28,29]. Gradually, scholars were not satisfied with the general event triggering method, and developed the dynamic event triggering mechanism. To further save the network bandwidth usage, this study introduces a dynamic event-triggered technique, where a dynamic event generator is utilized to detect whether the state is transmitted to the controller [30–32]. Make a comparison with the conventional static event-triggered approach, the dynamic type is more flexible because an internal dynamic variable is introduced based on the general static event-triggered method such that the dynamic judgement condition is agile. In [30,33], a dynamic event-triggered strategy was utilized to better filter communication signals. Several parameters including time-delay, disturbance and cyber nonlinearities bring challenges to our research.

Inspired by the above researches, $\mathcal{H}_\infty$ asynchronous filtering problems of MJS with cyber-attacks are investigated via dynamic event-triggered approach in this study. On one hand, there are so many parameters including disturbance and time-delay, the nonlinear cyber-attack, event-triggered parameters that increase the difficulty of the performance analysis and the dimension of matrices. On the other hand, there are major issues to be addressed, for example, how to deal with the nonlinear cyber-attack, how to establish the augmented system, and how to construct the stability condition. Some contributions of this paper are in the following:

- An internal dynamic variable is introduced into the general event-triggered condition to further save network resources in practical communication-linked environment.
- A low-conservative $\mathcal{H}_\infty$ filter is constructed subject to hidden Markovian model to characterize the asynchronous behavior between system and filter mode.
- The stochastic stability conditions are derived for the augmented filtering error time-delay system with cyber-attack nonlinearity and external disturbances to reduce conservativeness.

2. Problem formulation and preliminaries

2.1. System description

The MJS is provided as follows on a probability space $(\Omega, \mathcal{F}, \mathcal{P})$:

$$\begin{aligned} \dot{x}(t) &= A(r(t))x(t) + F(r(t))x(t-d(t)) + B(r(t))\omega(t), \\ y(t) &= C(r(t))x(t) + G(r(t))x(t-d(t)) + D(r(t))\omega(t), \\ z(t) &= E(r(t))x(t) \end{aligned} \tag{1}$$

where $x(t) \in \mathbf{R}^p$ is the state vector, $y(t) \in \mathbf{R}^q$ is the measured output, $z(t) \in \mathbf{R}^l$ is the estimated signal, and $d(t)$ is the time-varying delay which satisfies $0 < d(t) < h, 0 < \dot{d}(t) < \hat{d}$, $\omega(t) \in \mathbf{R}^m$ is the disturbance input which belongs to $\mathcal{L}_2 \in [0,\infty)$. $A(r(t)), B(r(t)), C(r(t)), D(r(t)), E(r(t)), F(r(t)), G(r(t))$ are known real constant matrices with compatible dimensions.

Markovian process $\{r(t), t \geq 0\}$ takes values in a finite set $\mathcal{N} = \{1, 2, \ldots, N\}$ with generator matrix $\Pi = \pi_{ij}, i, j \in \mathcal{N}$. The transition probability from mode i to mode j at time $t+\sigma$ is given by

$$Pr\{r(t+\sigma) = j | r(t) = i\} = \begin{cases} \pi_{ij}\sigma + o(\sigma), & \text{if } j \neq i \\ 1 + \pi_{ii}\sigma + o(\sigma), & \text{if } j = i \end{cases}$$

where $\sigma > 0$ and $\lim_{\sigma \to 0} o(\sigma)/\sigma = 0, \pi_{ij} > 0, j \neq i$ and $\pi_{ii} = -\sum_{j \neq i} \pi_{ij}$ for all $i \in \mathcal{N}$.

For each $r(t) = i (i \in \mathcal{N})$, we will denote the system matrices

$$\begin{aligned} \dot{x}(t) &= A_i x(t) + F_i x(t-d(t)) + B_i \omega(t) \\ y(t) &= C_i x(t) + G_i x(t-d(t)) + D_i \omega(t) \\ z(t) &= E_i x(t) \end{aligned} \tag{2}$$

2.2. Dynamic event-triggered method

Generally, a static event-triggered condition is given as follow to judge and execute the transmission of measurement output in the communication link:

$$\sigma_i \tilde{y}^T(t)\Omega_{1i}\tilde{y}(t) - e_y^T(t)\Omega_{2i}e_y(t) < 0, \tag{3}$$

where $e_y(t) \triangleq \bar{y}(t) - \tilde{y}(t)$ is the transmission error between the current sampled measured output $\tilde{y}(t) \triangleq y(sT), s = 0,1,2,\dots$ by sampling at the sampled period T and the latest transmitted state $\bar{y}(t) \triangleq y(s_lT), l = 0,1,2,\dots$. s_lT is the newest triggering instant $s_0, s_1, s_2, \dots, s_l, \dots \in \{0,1,2,\dots\}$. σ_i belongs to $[0,1)$ and Ω_{1i}, Ω_{2i} are weighting matrices to be designed. If (3) holds, signals will be sent successfully.

To filter signals and triggering events more flexibly, introduce an dynamic variable $\theta(t)$ based on the aforementioned event-triggered strategy (3)

$$\begin{aligned}\dot{\theta}(t) &= \sigma_i \tilde{y}^T(t)\Omega_{1i}\tilde{y}(t) - e_y^T(t)\Omega_{2i}e_y(t) - \rho\theta(t),\\ \theta(0) &= \theta_0 \geq 0,\end{aligned} \tag{4}$$

where $\rho > 0$. Therefore, a dynamic event generator $\mathrm{G}(\bullet)$ will be constructed as the variable

$$\mathrm{G}(y(t),\theta(t)) = \theta(t) + \mu\big(\sigma_i \tilde{y}^T(t)\Omega_{1i}\tilde{y}(t) - e_y^T(t)\Omega_{2i}e_y(t)\big), \tag{5}$$

and $\mu > 0$ is a known event-triggered parameter. $\theta(t)$ remains non-negative for a given initial parameter. As we can see from (5), if let $\theta(t)$ equal to zero, then the dynamic event-triggered method can be converted into the general one. From (4) and (5), it comes to

$$\dot{\theta}(t) \leq (\mu\rho + 1)\big(\sigma_i \tilde{y}^T(t)\Omega_{1i}\tilde{y}(t) - e_y^T(t)\Omega_{2i}e_y(t)\big). \tag{6}$$

System signals are transmitted only when $\mathrm{G}(y,\theta) < 0$, and the next triggering instant $s_{l+1}T$ is output as

$$s_{l+1}T = s_lT + \min_k \Big\{ kT | \mathrm{G}(y,\theta) < 0 \Big\}, k = 0,1,2,\dots. \tag{7}$$

Naturally, it indicates that there exists no triggering for any $t \in [s_lT, s_{l+1}T)$, and $\mathrm{G}(y,\theta) \geq 0$.

Assumption 1. For the triggering instant $\{s_0, s_1, s_2, \dots, s_l, \dots\}$, suppose that there exists a minimal release interval $\underline{\tau}$ to make the sequence s_lT meet with $s_{l+1}T - s_lT \geq \underline{\tau}$, where $\underline{\tau} > 0$ is a bound constant.

Remark 1. As is well known, Zeno behavior is indispensable for the event triggering mechanism. Assumption 1 limits the minimum release period and further avoids the infinite triggering of data within a finite time. That is to say, the Zeno phenomenon is avoided.

During the data transmission process, cyber-attacks occur occasionally. Let ϕ represent the cyber nonlinearity meeting with sector condition [34,35] as follows

$$\big(\phi(\eta) - K_1\eta\big)^T \big(\phi(\eta) - K_2\eta\big) \leq 0, \eta \in \mathbf{R}^q \tag{8}$$

where $K_1 \geq 0, K_2 \geq 0$ are constant parameters with $K_2 - K_1 > 0$.

Remark 2. As in [36], nonlinear functions are usually considered to belong to sectors $[K_1, K_2]$. The description of the nonlinearity in (8) is quite general including the usual Lipschitz condition as a special case. Note that both the control analysis and model reduction problems for systems with sector nonlinearities have been intensively studied, see e.g. [35,37,38].

The stochastic variable $\alpha(t)$ following the Bernoulli distribution is introduced to depict the random nonlinear cyber phenomenon, it has

$$\begin{cases} \alpha(t) = 1 & \text{the cyber-attacks are successful,} \\ \alpha(t) = 0 & \text{the cyber-attacks are insuccessful.} \end{cases} \tag{9}$$

and $\mathbf{E}\{\alpha(t) = 1\} = \alpha, \mathbf{E}\{\alpha(t) = 0\} = 1 - \alpha, \mathbf{E}\{(\alpha(t) - \alpha)^2\} = \hat{\alpha}^2, \hat{\alpha} \triangleq \sqrt{\alpha(1-\alpha)}$.

Affected by the cyber-attacks, the output signal $\hat{y}(t)$ transmitted by the ZOH is expressed by

$$\hat{y}(t) = \alpha(t)\bar{y}(t) + (1 - \alpha(t))\phi(\bar{y}(t)). \tag{10}$$

2.3. Asynchronous filter design

In this paper, considering the asynchronous phenomenon caused by clock signals out of sync between system and filter mode, a hidden Markovian chain $\delta(t), t$ is exploited to denote the mode of the filter taking values in a finite state space $\mathcal{M} = \{1,2,\dots,M\}$ and depend on $r(t)$ by the conditional probability matrix Δ

$$Pr\{\delta(t) = m | r(t) = i\} = \chi_{im}, \tag{11}$$

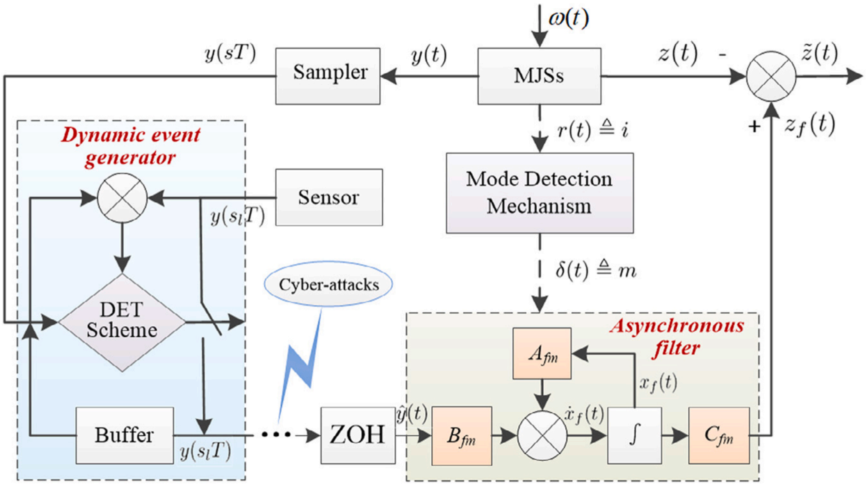

Fig. 1. The system structure block.

where $0 \le \chi_{im} \le 1, \sum_{m=1}^{M} \chi_{im} = 1$ for all $i \in \mathcal{N}$ and $m \in \mathcal{M}$.

Define an asynchronous filter of the following form

$$\begin{cases} \dot{x}_f(t) = A_f(\delta(t))x_f(t) + B_f(\delta(t))y_f(t) \\ z_f(t) = C_f(\delta(t))x_f(t) \end{cases} \tag{12}$$

where $x_f(t) \in \mathbf{R}^p$ is the state of the filter, $z_f(t) \in \mathbf{R}^l$ is the estimation of $z(t)$ and is also the output of filter, $y_f(t) \in \mathbf{R}^q$ is the input of the filter and is also the output signal of the ZOH, that is, $y_f(t) = \hat{y}(t)$. The matrices $A_{fm} \triangleq A_f(\delta(t) = m)$, $B_{fm} \triangleq B_f(\delta(t) = m)$, and $C_{fm} \triangleq C_f(\delta(t) = m)$ are the filter matrices with appropriate dimensions to be determined.

$$\begin{cases} \dot{x}_f(t) = A_{fm}x_f(t) + B_{fm}y_f(t) \\ z_f(t) = C_{fm}x_f(t) \end{cases}$$

Remark 3. Since the filter mode cannot be completely obtained through the system modes synchronization in practice, the transition probability (11) is naturally utilized to link the system and the filter modes. Then the augmented system will be regarded as a double random process. The hidden Markov models in [39] are introduced to describe the aforementioned asynchronous behavior.

The system filtering structure block is presented in Fig. 1. Including the states of filter (12) to augment the model of system (2), the filtering error system is obtained

$$\begin{aligned} \dot{\xi}(t) &= \xi_1(t) + (\alpha(t) - \alpha)\xi_2(t) \\ \tilde{z}(t) &= \bar{E}_i \xi(t) \end{aligned} \tag{13}$$

where

$$\begin{aligned}
\xi(t) &\triangleq \begin{bmatrix} x(t) \\ x_f(t) \end{bmatrix}, \tilde{z}(t) \triangleq z(t) - z_f(t), \\
\xi_1(t) &\triangleq \bar{A}_{im}\xi(t) + \bar{B}_{im}\xi(t-d(t)) + \bar{C}_{im}\omega(t) + \bar{D}_m e_y(t) + \bar{L}_m \phi(\bar{y}(t)), \\
\xi_2(t) &\triangleq \tilde{A}_{im}\xi(t) + \tilde{B}_{im}\xi(t-d(t)) + \tilde{C}_{im}\omega(t) + \tilde{D}_m e_y(t) + \tilde{L}_m \phi(\bar{y}(t)), \\
\bar{A}_{im} &\triangleq \begin{bmatrix} A_i & 0 \\ \alpha B_{fm} C_i & A_{fm} \end{bmatrix}, \bar{B}_{im} \triangleq \begin{bmatrix} F_i & 0 \\ \alpha B_{fm} G_i & 0 \end{bmatrix}, \bar{C}_{im} \triangleq \begin{bmatrix} B_i \\ \alpha B_{fm} D_i \end{bmatrix}, \\
\bar{D}_m &\triangleq \begin{bmatrix} 0 \\ \alpha B_{fm} \end{bmatrix}, \tilde{A}_{im} \triangleq \begin{bmatrix} 0 & 0 \\ B_{fm} C_i & 0 \end{bmatrix}, \tilde{B}_{im} \triangleq \begin{bmatrix} 0 & 0 \\ B_{fm} G_i & 0 \end{bmatrix}, \tilde{C}_{im} \triangleq \begin{bmatrix} 0 \\ B_{fm} D_i \end{bmatrix}, \\
\tilde{D}_m &\triangleq \begin{bmatrix} 0 \\ B_{fm} \end{bmatrix}, \tilde{L}_m \triangleq \begin{bmatrix} 0 \\ -B_{fm} \end{bmatrix}, \bar{L}_m \triangleq \begin{bmatrix} 0 \\ (1-\alpha) B_{fm} \end{bmatrix}, \bar{E}_i \triangleq \begin{bmatrix} E_i & -C_{fm} \end{bmatrix}.
\end{aligned}$$

Remark 4. From Fig. 1, we can notice that there exist two Markovian chains, one is the obvious Markovian jump system mode, and the other is the hidden asynchronous filter. Between the two modes, a mode detection mechanism is necessary to detect which filter is used under which subsystem. So the filter parameters A_{fm}, B_{fm}, C_{fm} seriously affect the filtering performance of the system. These will be designed in the next section.

Lemma 1 *([40]). Assume a time-varying function $d(t) \in (0, h]$ and a vector-valued function $\dot{\xi}(t) : (0, h] \to \mathbf{R}^n$, there exist matrices $Z = Z^T \in \mathbf{R}^{n\times n}$ and $S \in \mathbf{R}^{n\times n}$ such that $\begin{bmatrix} Z & \star \\ S^T & Z \end{bmatrix} \geq 0$. Then the following integral inequality holds:*

$$-h \int_{t-h}^{t} \dot{\xi}^T(s) Z \dot{\xi}(s) ds \leq \bar{\xi}^T(t) La \bar{\xi}(t). \tag{14}$$

where

$$\bar{\xi}(t) \triangleq \begin{bmatrix} \xi^T(t) & \xi^T(t-h) & \xi^T(t-d(t)) \end{bmatrix}^T,$$
$$La \triangleq \begin{bmatrix} -Z & \star & \star \\ -S^T & -Z & \star \\ Z+S^T & Z+S & -2Z-S-S^T \end{bmatrix}.$$

3. Main results

This section first provides the performance analysis of the augmented filtering error system (13). Simultaneously, considering nonlinear cyber-attacks and applying Lyapunov function and less conservative time-delay Lemma 1, the less conservative stochastic stability conditions of the system are established. Then, the asynchronous filter parameters are solved by a convex optimization problem and formulated.

Theorem 1. *For given scalars $\gamma > 0, \sigma_i \in [0,1), \alpha, \hat{\alpha} \triangleq \sqrt{\alpha(1-\alpha)}$, the system (13) is stochastically stable with an $\mathcal{H}_\infty$ performance gain γ if there exist symmetric positive definite matrices $P_i, Q, R, Z, \Omega_{1i}$, Ω_{2i}, and matrix S to make the following LMIs hold for $i \in \mathcal{N}, m \in \mathcal{M}$*

$$\bar{\Phi} = \begin{bmatrix} \bar{\Phi}_1 & \star & \star \\ \bar{\Phi}_2 & \bar{\Phi}_3 & \star \\ \bar{\Phi}_4 & \bar{\Phi}_5 & \bar{\Phi}_6 \end{bmatrix} < 0, \tag{15}$$

$$\begin{bmatrix} -P_i & \star \\ \bar{E}_i & -\gamma^2 I \end{bmatrix} \leq 0, \tag{16}$$

$$\begin{bmatrix} Z & \star \\ S^T & Z \end{bmatrix} \geq 0, \tag{17}$$

where

$$\bar{\Phi}_1 \triangleq \begin{bmatrix} \Phi_{11} & \star & \star \\ -S^T & \Phi_{22} & \star \\ \Phi_{31} & Z+S & \Phi_{33} \end{bmatrix}, \bar{\Phi}_2 \triangleq \begin{bmatrix} \Phi_{41} & 0 & \Phi_{43} \\ \Phi_{51} & 0 & \Phi_{53} \\ \Phi_{61} & 0 & \bar{G}_i \end{bmatrix}, \bar{\Phi}_3 \triangleq \begin{bmatrix} \Phi_{44} & \star & \star \\ \Phi_{54} & \Phi_{55} & \star \\ I & D_i & \Phi_{66} \end{bmatrix},$$
$$\bar{\Phi}_4 \triangleq \begin{bmatrix} hX_i\bar{A}_{im} & 0 & hX_i\bar{B}_{im} \\ h\hat{\alpha}X_i\tilde{A}_{im} & 0 & h\hat{\alpha}X_i\tilde{B}_{im} \\ \Phi_{91} & 0 & \Phi_{93} \end{bmatrix}, \bar{\Phi}_5 \triangleq \begin{bmatrix} hX_i\bar{D}_m & hX_i\bar{C}_{im} & hX_i\bar{L}_m \\ h\hat{\alpha}X_i\tilde{D}_m & h\hat{\alpha}X_i\tilde{C}_{im} & h\hat{\alpha}X_i\tilde{L}_m \\ 0 & \Phi_{95} & 0 \end{bmatrix},$$
$$\bar{\Phi}_6 \triangleq diag\{\Phi_{77}, \Phi_{88}, \Phi_{99}\},$$

with

$$\Phi_{11} \triangleq \sum_{m=1}^{M} \chi_{im}(P_i\bar{A}_{im} + \bar{A}_{im}^T P_i) + \sum_{j=1}^{N} \pi_{ij}P_j + Q + R - Z - \bar{C}_i^T K_1K_2\bar{C}_i,$$
$$X_i \triangleq \sum_{m=1}^{M} \chi_{im}P_i, \Phi_{22} \triangleq -Z-R, \Phi_{31} \triangleq \bar{B}_{im}^T X_i + Z + S^T - \bar{G}_i^T K_1K_2\bar{C}_i,$$
$$\Phi_{33} \triangleq -(1-\hat{d})Q - 2Z - S - S^T - \bar{G}_i^T K_1K_2\bar{G}_i, \Phi_{41} \triangleq \bar{D}_m^T X_i - K_1K_2\bar{C}_i,$$
$$\Phi_{51} \triangleq \bar{C}_{im}^T X_i - D_i^T K_1K_2\bar{C}_i, \Phi_{44} \triangleq -(\mu\rho+1)\Omega_{2i} - K_1K_2, \Phi_{43} \triangleq -K_1K_2\bar{G}_i,$$
$$\Phi_{53} \triangleq -D_i^T K_1K_2\bar{G}_i, \Phi_{54} \triangleq -K_1K_2D_i^T, \Phi_{61} \triangleq \bar{L}_m^T X_i + \bar{C}_i, \Phi_{66} \triangleq -(K_1K_2)^{-1}I,$$
$$\Phi_{77} = \Phi_{88} \triangleq Z - 2X_i, \Phi_{55} \triangleq -I - D_i^T K_1K_2D_i, \Phi_{91} \triangleq \sigma_i(\mu\rho+1)\Omega_{1i}\bar{C}_i,$$
$$\Phi_{93} \triangleq \sigma_i(\mu\rho+1)\Omega_{1i}\bar{G}_i, \Phi_{95} \triangleq \sigma_i(\mu\rho+1)\Omega_{1i}D_i, \Phi_{99} \triangleq -\sigma_i(\mu\rho+1)I.$$

Proof. Construct the Lyapunov function listed as follows

$$V(t,\xi(t),r(t),\delta(t),\theta(t)) = \sum_{n=1}^{5} V_n(t,\xi(t),r(t),\delta(t),\theta(t))$$
$$\triangleq \xi^T(t)P(r(t))\xi(t) + \int_{t-d(t)}^{t} \xi^T(s)Q\xi(s)ds$$

$$+\int_{t-h}^{t}\xi^T(s)R\xi(s)ds+h\int_{t-h}^{t}\int_{q}^{t}\dot{\xi}^T(s)Z\dot{\xi}(s)dsdq+\theta(t)$$

where $P_i(r(t)\triangleq i)>0, Q>0, R>0, Z>0$ are to be designed. Let $\mathcal{A}$ denote the weak infinitesimal generator. For $t\in[s_lT,s_{l+1}T)$, and $i\in\mathcal{N}, m\in\mathcal{M}$, we have

$$\begin{aligned}\mathbf{E}\big\{\mathcal{A}V(t,\xi(t),i,m,\theta(t))\big\} &= 2\xi^T(t)\Big(\sum_{m=1}^{M}\chi_{im}P_i\Big)\xi_1(t)+\xi^T(t)\Big(\sum_{j=1}^{N}\pi_{ij}P_j\Big)\xi(t)\\ &+\xi^T(t)Q\xi(t)-(1-\hat{d})\xi^T(t-d(t))Q\xi(t-d(t))\\ &+\xi^T(t)R\xi(t)-\xi^T(t-h)R\xi(t-h)\\ &+h^2{\xi_1}^T(t)Z\xi_1(t)+h^2\hat{\alpha}^2{\xi_2}^T(t)Z\xi_2(t)\\ &-h\int_{t-h}^{t}\dot{\xi}^T(s)Z\dot{\xi}(s)ds+\dot{\theta}(t),\end{aligned}\tag{18}$$

where $h^2{\xi_1}^T(t)Z\xi_1(t)=\psi^T(t)\Theta_1\psi(t), h^2\hat{\alpha}^2{\xi_2}^T(t)Z\xi_2(t)=\psi^T(t)\Theta_2\psi(t)$ with

$$\psi(t)\triangleq[\xi^T(t)\ \xi^T(t-h)\ \xi^T(t-d(t))\ e_y^T(t)\ \omega^T(t)\ \phi^T(\bar{y}(t))]^T,$$

$$\Theta_1\triangleq\begin{bmatrix}h\bar{A}_{im}^T\\0\\h\bar{B}_{im}^T\\h\bar{D}_m^T\\h\bar{L}_m^T\\h\bar{C}_{im}^T\end{bmatrix}Z\begin{bmatrix}h\bar{A}_{im}^T\\0\\h\bar{B}_{im}^T\\h\bar{D}_m^T\\h\bar{L}_m^T\\h\bar{C}_{im}^T\end{bmatrix}^T,\Theta_2\triangleq\begin{bmatrix}h\hat{\alpha}\tilde{A}_{im}^T\\0\\h\hat{\alpha}\tilde{B}_{im}^T\\h\hat{\alpha}\tilde{D}_m^T\\h\hat{\alpha}\tilde{L}_m^T\\h\hat{\alpha}\tilde{C}_{im}^T\end{bmatrix}Z\begin{bmatrix}h\hat{\alpha}\tilde{A}_{im}^T\\0\\h\hat{\alpha}\tilde{B}_{im}^T\\h\hat{\alpha}\tilde{D}_m^T\\h\hat{\alpha}\tilde{L}_m^T\\h\hat{\alpha}\tilde{C}_{im}^T\end{bmatrix}^T,$$

Considering condition (6), it follows that

$$\begin{aligned}\dot{\theta}(t)&\le(\mu\rho+1)\big(\sigma_i\tilde{y}^T(t)\Omega_{1i}\tilde{y}(t)-e_y^T(t)\Omega_{2i}e_y(t)\big)\\ &\le\sigma_i(\mu\rho+1)\big[\bar{C}_i\xi(t)+\bar{G}_i\xi(t-d(t))+D_i\omega(t)\big]^T\Omega_{1i}\big[\bar{C}_i\xi(t)+\bar{G}_i\xi(t-d(t))+D_i\omega(t)\big]\\ &\quad-(\mu\rho+1)e_y^T(t)\Omega_{2i}e_y(t),\end{aligned}$$

where $\bar{C}_i\triangleq\begin{bmatrix}C_i & 0\end{bmatrix}, \bar{G}_i\triangleq\begin{bmatrix}G_i & 0\end{bmatrix}$.

According to $\varsigma(t)=\big(\phi(\eta)-K_1\eta\big)^T\big(\phi(\eta)-K_2\eta\big)\le 0$, and Lemma 1, for $\omega(t)\neq 0$ and belongs to $\mathcal{L}_2[0,\infty)$ and under zero initial condition, it comes to

$$\begin{aligned}\mathrm{J}&=\mathbf{E}\left\{\int_0^t\big[\mathcal{A}V(\bullet)-\omega^T(s)\omega(s)\big]ds\right\}\\ &\le\mathbf{E}\left\{\int_0^t\big[\mathcal{A}V(\bullet)-\omega^T(s)\omega(s)-\varsigma(s)\big]ds\right\}\\ &\le\mathbf{E}\left\{\int_0^t\psi^T(s)\Phi\psi(s)ds\right\},\end{aligned}$$

where

$$\Phi=\begin{bmatrix}\Phi_1&\star&\star\\\Phi_2&\Phi_3&\star\\\Phi_4&\Phi_5&\Phi_6\end{bmatrix}<0,\tag{19}$$

with

$$\begin{aligned}\Phi_1&=\bar{\Phi}_1,\Phi_2=\bar{\Phi}_2,\Phi_3=\bar{\Phi}_3,\Phi_6\triangleq diag\{-Z,-Z,\Phi_{99}\},\\ \Phi_4&\triangleq\begin{bmatrix}h\bar{A}_{im}&0&h\bar{B}_{im}\\h\hat{\alpha}\tilde{A}_{im}&0&h\hat{\alpha}\tilde{B}_{im}\\\Phi_{91}&0&\Phi_{93}\end{bmatrix},\Phi_5\triangleq\begin{bmatrix}h\bar{D}_m&h\bar{C}_{im}&h\bar{L}_m\\h\hat{\alpha}\tilde{D}_m&h\hat{\alpha}\tilde{C}_{im}&h\hat{\alpha}\tilde{L}_m\\0&\Phi_{95}&0\end{bmatrix},\end{aligned}$$

and other terms are defined in Theorem 1. Performing a congruence transformation on (19) by $diag\{I,I,Tran\}$, $Tran\triangleq diag\{X_iZ^{-1},X_iZ^{-1},I\}$ and

$$(X_i-Z)Z^{-1}(X_i-Z)^T\ge 0,$$

we have $\bar{\Phi}<0$ defined in (15). That is, J <0 for $\omega(t)\neq 0$ and belongs to $\mathcal{L}_2[0,\infty)$ and under zero initial condition, it implies that

$$\mathbf{E}\left\{\xi^T(t)P_i\xi(t)\right\}\le\mathbf{E}\left\{V(\bullet)\right\}<\mathbf{E}\left\{\int_0^t\omega^T(s)\omega(s)ds\right\}.\tag{20}$$

By applying Schur complement, (16) yields

$$\bar{E}_i^T \bar{E}_i \leq \gamma^2 P_i. \tag{21}$$

Combining (20) with (21), the following can be concluded

$$\begin{aligned}\mathbf{E}\left\{\tilde{z}^T(t)\tilde{z}(t)\right\} &= \mathbf{E}\left\{\xi^T(t)\bar{E}_i^T\bar{E}_i\xi(t)\right\}\\ &\leq \gamma^2\mathbf{E}\left\{\xi^T(t)P_i\xi(t)\right\}\\ &\leq \gamma^2\mathbf{E}\left\{\int_0^t \omega^T(s)\omega(s)ds\right\}\\ &\leq \gamma^2\mathbf{E}\left\{\int_0^\infty \omega^T(s)\omega(s)ds\right\}.\end{aligned} \tag{22}$$

Thus the $\mathcal{H}_\infty$ performance with gain γ has been established. Stability analysis under $\omega(t) = 0$ can be easily proved, so here omits the proof.

Theorem 2. *For given scalars $\gamma > 0, \sigma_i \in [0,1), \alpha, \hat{\alpha} \triangleq \sqrt{\alpha(1-\alpha)}$, if there exist matrices $P_{1i} > 0, U_i > 0, U_{ij}, V_{ij} > 0, Q_1 > 0, \bar{Q}_2 > 0, R_1 > 0, \bar{R}_2 > 0, Z_1 > 0, \bar{Z}_2 > 0, \Omega_{1i} > 0, \Omega_{2i} > 0$, and $S_{11}, \bar{S}_{12}, \bar{S}_{21}, \bar{S}_{22}$, satisfying the following LMIs for $i \in \mathcal{N}, m \in \mathcal{M}$,*

$$\Xi \triangleq \begin{bmatrix} \Xi_1 & \star & \star & \star & \star \\ \Xi_2 & \Xi_3 & \star & \star & \star \\ \Xi_4 & \Xi_5 & \Xi_6 & \star & \star \\ \Xi_7 & 0 & \Xi_8 & \Xi_9 & \star \\ \Xi_{10} & 0 & \Xi_{11} & \Xi_{12} & \Xi_{13} \end{bmatrix} < 0, \tag{23}$$

$$\begin{bmatrix} -P_{1i} & \star & \star \\ -U_i & -U_i & \star \\ E_i & -\sum_{m=1}^{M}\chi_{im}\bar{C}_{fim} & -\gamma^2 I \end{bmatrix} \leq 0, \tag{24}$$

$$\begin{bmatrix} Z_1 & \star & \star & \star \\ 0 & \bar{Z}_2 & \star & \star \\ S_{11}^T & \bar{S}_{21}^T & Z_1 & \star \\ \bar{S}_{12}^T & \bar{S}_{22}^T & 0 & \bar{Z}_2 \end{bmatrix} \geq 0, \tag{25}$$

$$\begin{bmatrix} P_{1i} & \star \\ U_i & U_i \end{bmatrix} > 0, \tag{26}$$

where

$$\Xi_1 = \begin{bmatrix} \Xi_1^1 & \star \\ \Xi_2^1 & \Xi_2^2 \end{bmatrix}, \Xi_2 \triangleq \begin{bmatrix} -S_{11}^T & -\bar{S}_{21}^T, \\ -\bar{S}_{12}^T & -\bar{S}_{22}^T \end{bmatrix}, \Xi_3 = diag\left\{-Z_1 - R_1, -\bar{Z}_2 - \bar{R}_2\right\},$$

$$\Xi_4 = \begin{bmatrix} \Xi_5^1 & \Xi_5^2 \\ \bar{S}_{12}^T & \bar{Z}_2 + \bar{S}_{22}^T \end{bmatrix}, \Xi_5 \triangleq \begin{bmatrix} \Xi_5^3 & \bar{S}_{12} \\ \bar{S}_{21} & \Xi_6^4 \end{bmatrix}, \Xi_6 = \begin{bmatrix} \Xi_5^5 & \star \\ -\bar{S}_{21} - \bar{S}_{12}^T & \Xi_6^6 \end{bmatrix},$$

$$\Xi_7 = \begin{bmatrix} \Xi_7^1 & \Xi_7^2 \\ \Xi_8^1 & \Xi_8^2 \\ \Xi_9^1 & \Xi_9^2 \end{bmatrix}, \Xi_8 = \begin{bmatrix} \Xi_7^5 & 0 \\ \Xi_8^5 & 0 \\ G_i & 0 \end{bmatrix}, \Xi_9 \triangleq \begin{bmatrix} \Xi_7^7 & \star & \star \\ \Xi_8^7 & \Xi_8^8 & \star \\ I & D_i & \Xi_9^9 \end{bmatrix},$$

$$\Xi_{10} = \begin{bmatrix} \Xi_{10}^1 & \Xi_{10}^2 \\ \Xi_{11}^1 & \Xi_{11}^2 \\ \Xi_{12}^1 & 0 \\ \Xi_{13}^1 & 0 \\ \Xi_{14}^1 & 0 \end{bmatrix}, \Xi_{11} \triangleq \begin{bmatrix} \Xi_{10}^5 & 0 \\ \Xi_{11}^5 & 0 \\ \Xi_{12}^5 & 0 \\ \Xi_{13}^5 & 0 \\ \Xi_{14}^5 & 0 \end{bmatrix}, \Xi_{12} = \begin{bmatrix} \Xi_{10}^7 & \Xi_{10}^8 & \Xi_{10}^9 \\ \Xi_{11}^7 & \Xi_{11}^8 & \Xi_{11}^9 \\ \Xi_{12}^7 & \Xi_{12}^8 & \Xi_{12}^9 \\ \Xi_{13}^7 & \Xi_{13}^8 & \Xi_{13}^9 \\ 0 & \Xi_{14}^8 & 0 \end{bmatrix},$$

$$\Xi_{13} = \begin{bmatrix} \Xi_{10}^{10} & \star & \star & \star & \star \\ 0 & \Xi_{11}^{11} & \star & \star & \star \\ 0 & 0 & \Xi_{12}^{12} & \star & \star \\ 0 & 0 & \Xi_{13}^{12} & \Xi_{13}^{13} & \star \\ 0 & 0 & 0 & 0 & \Xi_{14}^{14} \end{bmatrix},$$

with

$$
\begin{aligned}
\Xi_1^1 &\triangleq \sum_{m=1}^{M} \chi_{im}(\alpha\bar{B}_{fim}C_i+\alpha C_i^T B_{fim}^T)+P_{1i}A_i+A_i^T P_{1i}+\sum_{j=1}^{N}\pi_{ij}P_{1j}+Q_1+R_1-Z_1-C_i^T K_1 K_2 C_i,\\
\Xi_2^1 &\triangleq \sum_{m=1}^{M}\chi_{im}(\alpha\bar{B}_{fim}C_i+\bar{A}_{fim}^T)+U_iA_i+\sum_{j=1}^{N}\pi_{ij}U_{ij}, \Xi_{14}^{14} \triangleq -\sigma_i(\mu\rho+1)I,\\
\Xi_2^2 &\triangleq \sum_{m=1}^{M}\chi_{im}(\bar{A}_{fim}+\bar{A}_{fim}^T)+\sum_{j=1}^{N}\pi_{ij}V_{ij}+\bar{Q}_2+\bar{R}_2-\bar{Z}_2, \Xi_{14}^1 \triangleq \sigma_i(\mu\rho+1)\Omega_{1i}C_i,\\
\Xi_5^1 &\triangleq \sum_{m=1}^{M}\chi_{im}\alpha G_i^T\bar{B}_{fim}^T+F_i^TP_{1i}+Z_1+S_{11}^T-G_i^TK_1K_2C_i, \Xi_{11}^{11}=\Xi_{13}^{13}\triangleq \bar{Z}_2-2U_i,\\
\Xi_5^2 &\triangleq \sum_{m=1}^{M}\chi_{im}\alpha G_i^T\bar{B}_{fim}^T+F_i^TU_i+\bar{S}_{21}^T, \Xi_5^3\triangleq Z_1+S_{11}, \Xi_6^4\triangleq \bar{Z}_2+\bar{S}_{22}, \Xi_9^9\triangleq -(K_1K_2)^{-1}I,\\
\Xi_5^5 &\triangleq -(1-\hat{d})Q_1-2Z_1-S_{11}-S_{11}^T-G_i^TK_1K_2G_i, \Xi_6^6\triangleq -(1-\hat{d})\bar{Q}_2-2\bar{Z}_2-\bar{S}_{22}-\bar{S}_{22}^T,\\
\Xi_7^1 &\triangleq \sum_{m=1}^{M}\chi_{im}\bar{B}_{fim}^T-K_1K_2C_i, \Xi_7^2\triangleq \sum_{m=1}^{M}\chi_{im}\alpha\bar{B}_{fim}^T, \Xi_7^5\triangleq -K_1K_2G_i,\\
\Xi_7^7 &\triangleq -(\mu\rho+1)\Omega_{2i}-K_1K_2I, \Xi_8^1\triangleq \sum_{m=1}^{M}\chi_{im}\alpha D_i^T\bar{B}_{fim}^T+B_i^TP_{1i}-D_i^TK_1K_2C_i,\\
\Xi_8^2 &\triangleq \sum_{m=1}^{M}\chi_{im}\alpha D_i^T\bar{B}_{fim}^T+B_i^TU_i, \Xi_8^5\triangleq -D_i^TK_1K_2G_i, \Xi_{10}^5\triangleq hP_{1i}F_i+\sum_{m=1}^{M}\chi_{im}h\alpha\bar{B}_{fim}G_i,\\
\Xi_8^8 &\triangleq -I-D_i^TK_1K_2D_i, \Xi_9^1\triangleq \sum_{m=1}^{M}\chi_{im}(1-\alpha)\bar{B}_{fim}^T+C_i, \Xi_9^2\triangleq \sum_{m=1}^{M}\chi_{im}(1-\alpha)\bar{B}_{fim}^T,\\
\Xi_{10}^1 &\triangleq hP_{1i}A_i+\sum_{m=1}^{M}\chi_{im}h\alpha\bar{B}_{fim}C_i, \Xi_{10}^2\triangleq \sum_{m=1}^{M}\chi_{im}h\bar{A}_{fim}, \Xi_8^7\triangleq -K_1K_2D_i^T,\\
\Xi_{10}^8 &\triangleq hP_{1i}B_i+\sum_{m=1}^{M}\chi_{im}h\alpha\bar{B}_{fim}D_i, \Xi_{10}^9\triangleq \sum_{m=1}^{M}\chi_{im}h(1-\alpha)\bar{B}_{fim}, \Xi_{10}^{10}=\Xi_{12}^{12}\triangleq Z_1-2P_{1i},\\
\Xi_{10}^7 &\triangleq \sum_{m=1}^{M}\chi_{im}h\alpha\bar{B}_{fim}, \Xi_{11}^1\triangleq hU_iA_i+\sum_{m=1}^{M}\chi_{im}\alpha\bar{B}_{fim}C_i, \Xi_{11}^2\triangleq \sum_{m=1}^{M}\chi_{im}h\bar{A}_{fim},\\
\Xi_{11}^5 &\triangleq hU_iF_i+\sum_{m=1}^{M}\chi_{im}\alpha\bar{B}_{fim}G_i, \Xi_{14}^8\triangleq \sigma_i(\mu\rho+1)\Omega_{1i}D_i, \Xi_{11}^7\triangleq \sum_{m=1}^{M}\chi_{im}h\alpha\bar{B}_{fim},\\
\Xi_{11}^9 &\triangleq \sum_{m=1}^{M}\chi_{im}h(1-\alpha)\bar{B}_{fim}, \Xi_{12}^7\triangleq \sum_{m=1}^{M}\chi_{im}h\hat{\alpha}\bar{B}_{fim}, \Xi_{11}^{10}=\Xi_{13}^{12}\triangleq -2\sum_{m=1}^{M}\chi_{im}U_i,\\
\Xi_{12}^1 &\triangleq \sum_{m=1}^{M}\chi_{im}h\hat{\alpha}\bar{B}_{fim}C_i, \Xi_{12}^5\triangleq \sum_{m=1}^{M}\chi_{im}h\hat{\alpha}\bar{B}_{fim}G_i, \Xi_{12}^8\triangleq \sum_{m=1}^{M}\chi_{im}h\hat{\alpha}\bar{B}_{fim}D_i,\\
\Xi_{12}^9 &\triangleq -\sum_{m=1}^{M}\chi_{im}h\hat{\alpha}\bar{B}_{fim}, \Xi_{13}^1\triangleq \sum_{m=1}^{M}\chi_{im}h\hat{\alpha}\bar{B}_{fim}C_i, \Xi_{13}^5\triangleq \sum_{m=1}^{M}\chi_{im}h\hat{\alpha}\bar{B}_{fim}G_i,\\
\Xi_{13}^7 &\triangleq \sum_{m=1}^{M}\chi_{im}h\hat{\alpha}\bar{B}_{fim}, \Xi_{13}^8\triangleq \sum_{m=1}^{M}\chi_{im}h\hat{\alpha}\bar{B}_{fim}D_i, \Xi_{13}^9\triangleq -\sum_{m=1}^{M}\chi_{im}h\hat{\alpha}\bar{B}_{fim},\\
\Xi_{13}^{12} &\triangleq -\sum_{m=1}^{M}\chi_{im}U_i, \Xi_{11}^8\triangleq hU_iB_i+\sum_{m=1}^{M}\chi_{im}h\alpha\bar{B}_{fim}D_i, \Xi_{14}^5\triangleq \sigma_i(\mu\rho+1)\Omega_{1i}G_i.
\end{aligned}
$$

Then, there exists a desired asynchronous filter to make the event-based augmented system (13) stochastically stable with an $\mathcal{H}_\infty$ performance gain γ. Besides, if the aforementioned conditions are feasible, the filter parameters can be given by

$$
\begin{bmatrix} A_{fm} & B_{fm} \\ C_{fm} & 0 \end{bmatrix} = \begin{bmatrix} U_i^{-1} & 0 \\ 0 & I \end{bmatrix} \begin{bmatrix} \bar{A}_{fim} & \bar{B}_{fim} \\ \bar{C}_{fim} & 0 \end{bmatrix} \tag{27}
$$

Proof. First, set

$$
P_i \triangleq \begin{bmatrix} P_{1i} & \star \\ P_{3i} & P_{2i} \end{bmatrix}, Q \triangleq \begin{bmatrix} Q_1 & \\ & Q_2 \end{bmatrix}, R \triangleq \begin{bmatrix} R_1 & \\ & R_2 \end{bmatrix}, Z \triangleq \begin{bmatrix} Z_1 & \\ & Z_2 \end{bmatrix}, S \triangleq \begin{bmatrix} S_{11} & S_{12} \\ S_{21} & S_{22} \end{bmatrix},
$$

where P_{2i} and P_{3i} are invertible. Define the following invertible matrix $\mathcal{W} \triangleq diag\{I, P_{2i}^{-1}P_{3i}\}$,

$$\begin{aligned} U_i &\triangleq P_{3i}^T P_{2i}^{-1} P_{3i}, \bar{Q}_2 \triangleq P_{3i}^T P_{2i}^{-1} Q_2 P_{2i}^{-1} P_{3i}, \bar{R}_2 \triangleq P_{3i}^T P_{2i}^{-1} R_2 P_{2i}^{-1} P_{3i}, \\ \bar{Z}_2 &\triangleq P_{3i}^T P_{2i}^{-1} Z_2 P_{2i}^{-1} P_{3i}, \bar{S}_{12} \triangleq S_{12} P_{2i}^{-1} P_{3i}, \bar{S}_{21} \triangleq P_{3i}^T P_{2i}^{-1} S_{21}, \bar{S}_{22} \triangleq P_{3i}^T P_{2i}^{-1} S_{22} P_{2i}^{-1} P_{3i}, \\ \bar{A}_{fim} &\triangleq P_{3i}^T A_{fm} P_{2i}^{-1} P_{3i}, \bar{B}_{fim} \triangleq P_{3i}^T B_{fm}, \bar{C}_{fim} \triangleq C_{fm} P_{2i}^{-1} P_{3i}, \end{aligned} \tag{28}$$

and for $j \neq i, j = 1, 2, \ldots, N$,

$$U_{ij} \triangleq P_{3i}^T P_{2i}^{-1} P_{3j}, V_{ij} \triangleq P_{3i}^T P_{2i}^{-1} P_{2j} P_{2i}^{-1} P_{3i}.$$

Then, pre-and post-multiplying (15), (16) and (17) by $diag\{\{\mathcal{W},\mathcal{W},\mathcal{W}\},\{I,I,I\},\{\mathcal{W},\mathcal{W},I\}\}$, $diag\left\{\ \sum_{m=1}^{M}\chi_{im}\mathcal{W},\ I\ \right\}$ and $diag\{\mathcal{W},\mathcal{W}\}$, we readily obtain (23), (24) and (25), respectively. In addition, from $\mathcal{W}^T P_i \mathcal{W} > 0$, we have (26).

From (28), it gets

$$\begin{bmatrix} A_{fm} & B_{fm} \\ C_{fm} & 0 \end{bmatrix} = \begin{bmatrix} P_{3i}^{-T} & 0 \\ 0 & I \end{bmatrix} \begin{bmatrix} \bar{A}_{fim} & \bar{B}_{fim} \\ \bar{C}_{fim} & 0 \end{bmatrix} \begin{bmatrix} P_{3i}^{-1}P_{2i} & 0 \\ 0 & I \end{bmatrix}.$$

Simultaneously, from (12), we can denote the transfer function from the measured output $y_f(t)$ to the estimated signal $z_f(t)$:

$$\begin{aligned} T_{z_f y} &= C_{fm}(sI - A_{fm})^{-1} B_{fm} \\ &= \bar{C}_{fim} P_{3i}^{-1} P_{2i} (sI - P_{3i}^{-T} \bar{A}_{fim} P_{3i}^{-1} P_{2i})^{-1} P_{3i}^{-T} \bar{B}_{fim} \\ &= \bar{C}_{fim} (sI - U_i^{-1} \bar{A}_{fim})^{-1} U_i^{-1} \bar{B}_{fim}. \end{aligned} \tag{29}$$

Hence, we can obtain the conclusion from (29) that the filter parameters (12) will be established by (27). Thus, the proof has been completed.

Remark 5. The parameters of the asynchronous filter is given by (27). These LMIs (23)–(25) seem to be bulky and cumbersome since so many issues are involved such as time-delay, disturbance, event-triggered variable and filter variable and so on in this study. Once these inequalities are input by Matlab/LMI Toolbox, some relevant parameters can be output.

4. Simulation results

This part provides two simulations to show the effectiveness of the proposed theoretical technique.

Example 1. Given the following MJS with $N = 2$:
Mode 1:

$$\begin{aligned} A_1 &= \begin{bmatrix} -0.28 & -0.01 & -0.02 \\ -0.2 & -0.25 & -0.29 \\ 0.03 & -0.04 & -0.23 \end{bmatrix}, F_1 = \begin{bmatrix} 0.1 & 0.2 & -0.2 \\ 0.1 & -0.1 & 0.3 \\ 0.2 & 0.3 & 0.01 \end{bmatrix}, B_1 = \begin{bmatrix} -2.02 \\ 2.83 \\ 1.39 \end{bmatrix}, \\ C_1 &= \begin{bmatrix} 0.3 & 0.11 & 0.1 \end{bmatrix}, G_1 = \begin{bmatrix} 0.31 & 0.12 & 0.2 \end{bmatrix}, D_1 = 0.2, E_1 = \begin{bmatrix} 0.1 & 0.1 & 0.1 \end{bmatrix}, \end{aligned}$$

Mode 2:

$$\begin{aligned} A_2 &= \begin{bmatrix} -0.3 & 0 & 0.1 \\ -0.59 & -0.24 & 0.02 \\ 0.1 & -0.06 & -0.68 \end{bmatrix}, F_2 = \begin{bmatrix} 0.11 & 0 & 0.2 \\ -0.01 & -0.11 & 0.2 \\ 0.21 & 0.31 & 0.22 \end{bmatrix}, B_2 = \begin{bmatrix} 2.04 \\ -2.25 \\ -0.73 \end{bmatrix}, \\ C_2 &= \begin{bmatrix} 0.25 & 0.3 & 0.2 \end{bmatrix}, G_2 = \begin{bmatrix} 0.11 & 0.12 & 0.1 \end{bmatrix}, D_2 = 1.5, E_2 = \begin{bmatrix} 0.2 & 0.19 & 0.2 \end{bmatrix}, \end{aligned}$$

with the disturbance input $\omega(t) = \frac{10\sin(0.5\pi t)}{1+t^2}$ and the cyber nonlinearity is selected as $\phi(\eta) = \frac{K_1+K_2}{2}\eta + \frac{K_2-K_1}{2}\sin(\eta)$ shown in Fig. 2, where $K_1 = 4, K_2 = 5$. In this example, the transition probability of MJS and the asynchronous filter are set as

$$\Pi = \begin{bmatrix} -0.6 & 0.6 \\ 0.4 & -0.4 \end{bmatrix}, \Delta = \begin{bmatrix} 0.45 & 0.55 \\ 0.73 & 0.27 \end{bmatrix},$$

respectively. Select the event-triggered parameters $\sigma_1 = 0.6, \sigma_2 = 0.5$. By calculating Theorem 2 under LMI Toolbox/MATLAB, filter parameters are obtained

$$\begin{aligned} A_{f1} &= \begin{bmatrix} -0.3876 & 0.0547 & -0.0922 \\ -0.0552 & -0.4363 & 0.0221 \\ -0.0373 & 0.0031 & -0.3976 \end{bmatrix}, A_{f2} = \begin{bmatrix} -0.2222 & 0.0383 & 0.0022 \\ 0.0171 & -0.3440 & -0.0421 \\ -0.0223 & 0.0006 & -0.2040 \end{bmatrix}, \\ B_{f1} &= \begin{bmatrix} -0.0670 & 0.1196 & -0.0003 \end{bmatrix}^T, B_{f2} = \begin{bmatrix} -0.1819 & 0.5266 & -0.0236 \end{bmatrix}^T, \\ C_{f1} &= \begin{bmatrix} -0.0531 & -0.0382 & -0.0511 \end{bmatrix}, C_{f2} = \begin{bmatrix} -0.0798 & -0.0491 & -0.0558 \end{bmatrix}. \end{aligned}$$

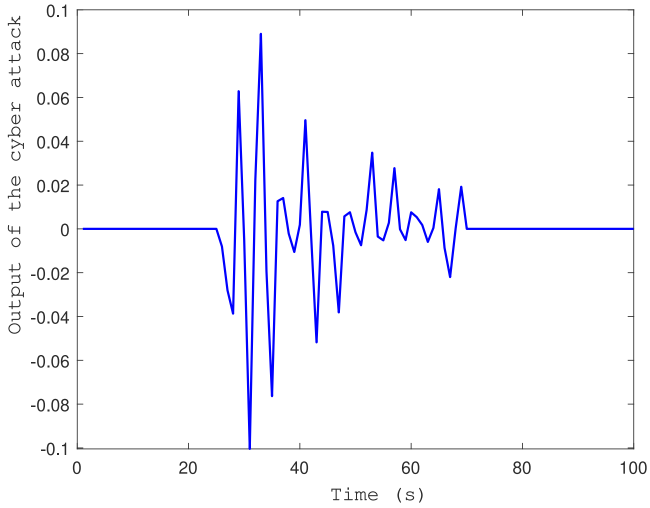

Fig. 2. The output of the cyber-attack.

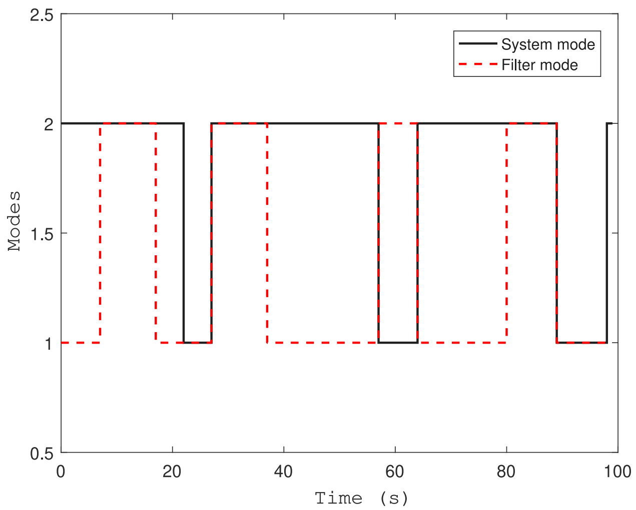

Fig. 3. The system and filter modes.

The switching signal of the system (which is generated randomly) and the filter mode are both given in Fig. 3. During the network communication, the packet dropouts of the cyber-attacks $\alpha(t)$ satisfy $\mathbf{E}\{\alpha(t) = 1\} = \alpha = 0.45$ (which is presented in Fig. 4). The simulation results are presented as Figs. 5–9. Fig. 5 depicts the actual system states before cyber-attack while Fig. 6 shows the states of the asynchronous filter with cyber-attack. The internal dynamic variable $\theta(t)$ of the dynamic event-triggered approach is presented in Fig. 7. The release instants and intervals under the proposed dynamic scheme is presented in Fig. 8, while the static one is shown in Fig. 9. It can be easily get that the transmits percentage can be significantly reduced from 54% to 22%. The figures show that the proposed method can filter signals and triggering events more flexibly.

Example 2. In the industrial manufacturing environment, manipulators are widely used. When the manipulator is used to do some repetitive work, such as logistics handling, welding chips and so on, the working process of the manipulator can be seen as a Markov jump system. Borrowed the single-link robot arm example from [13], without considering the control input, its state space representation is listed as followings

$$J_i\ddot{\phi} = -gL\left(\frac{1}{2}m+M_i\right)\sin(\phi(t)) - D(t)\dot{\phi}(t) + L\omega(t).$$

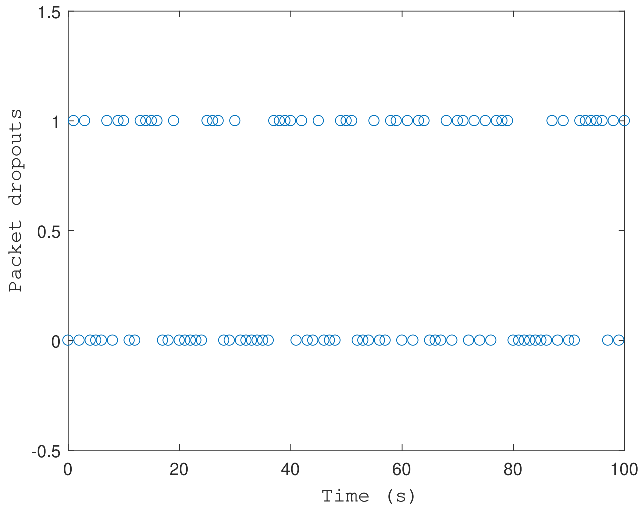

Fig. 4. The packet dropout $\alpha(t)$ of cyber-attacks.

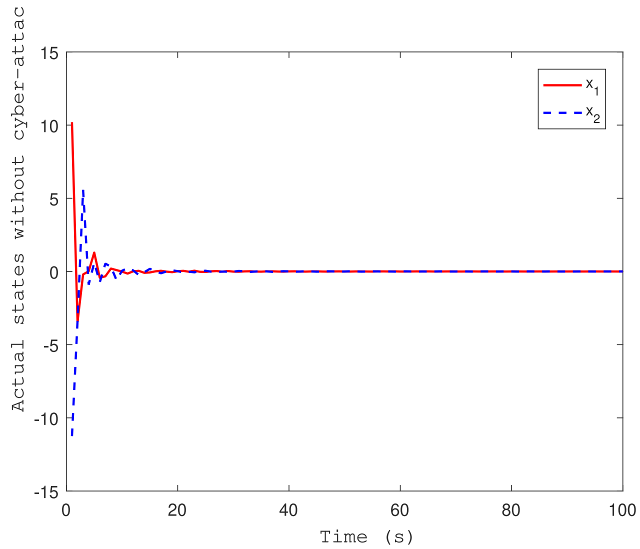

Fig. 5. Actual states without cyber-attack.

Let $x_1(t) = \phi(t)$ and $x_2(t) = \dot{\phi}$ to linearize the system above, we have

$$\dot{x}(t)=\begin{bmatrix} 0 & 1 \\ -\frac{gL}{J_i}\left(\frac{1}{2}m+M_i\right) & -\frac{D_0}{J_i} \end{bmatrix}x(t)+\begin{bmatrix} 0 \\ -\frac{L}{J_i} \end{bmatrix}\omega(t).$$

The relevant parameter selection can be referred to the literature [13]. Some simulation results are presented in Figs. 10–13. Fig. 10 shows the asynchronous behavior between the system and the filter. Fig. 11 plots the filtering curves, especially the nonlinear cyber attack at 45–75 s. Figs. 12, 13 depict the release instants and intervals and the transmits percentage can be significantly reduced from 69% to 12%. As we can see from Figs. 2 and 11, the attack duration is 25 to 40 s and 45 to 75 s during system data transmission, respectively. Before the actual system states are stable, while after suffering from cyber-attack, a slight disturbance occurs on the filtered states but it leveled off quickly.

Remark 6. From the resulting figures shown above, when there exists asynchronous phenomenon between the system and filter (Figs. 3,10), with the nonlinear cyber-attack Fig. 2, the designed filter of this paper can effectively filter disturbance and the nonlinear cyber-attacks (Figs. 6, 11). From Figs. 8, 9 and Figs. 12, 13, it can be concluded that dynamic event triggering can greatly reduce network bandwidth utilization compared with the static event triggering. All of these verify the proposed algorithm. Although these

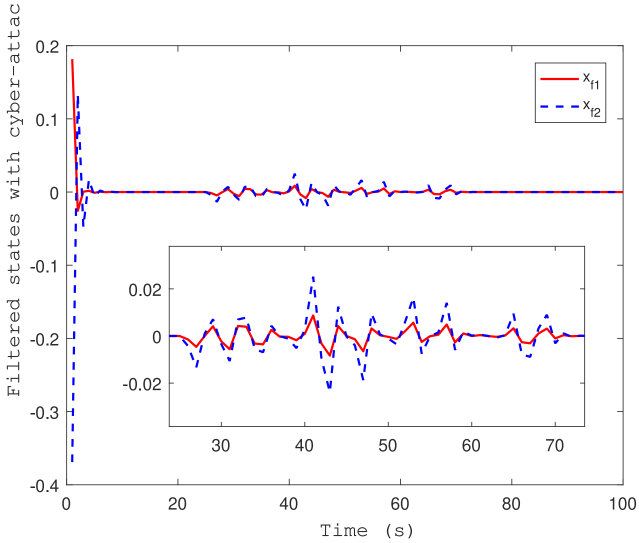

Fig. 6. Filtered states with cyber-attack.

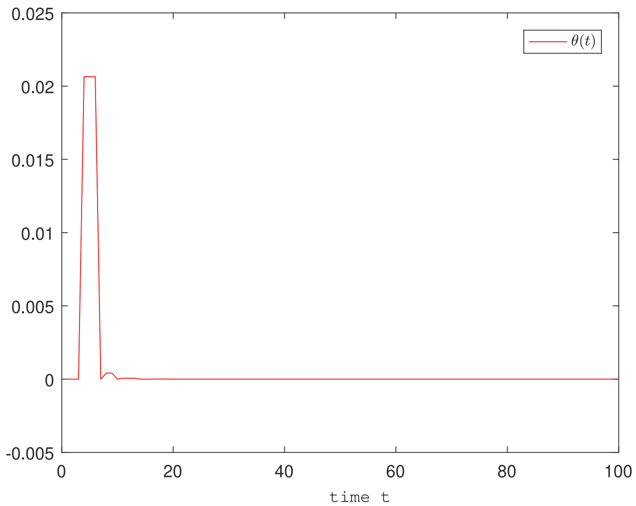

Fig. 7. The internal dynamic variable $\theta(t)$.

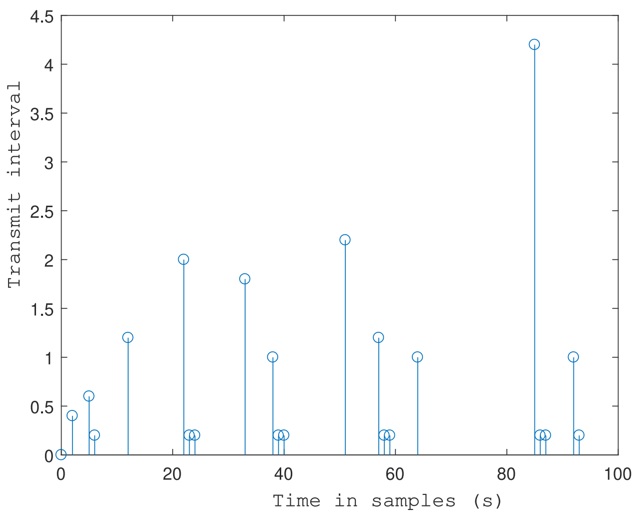

Fig. 8. The dynamic event interval.

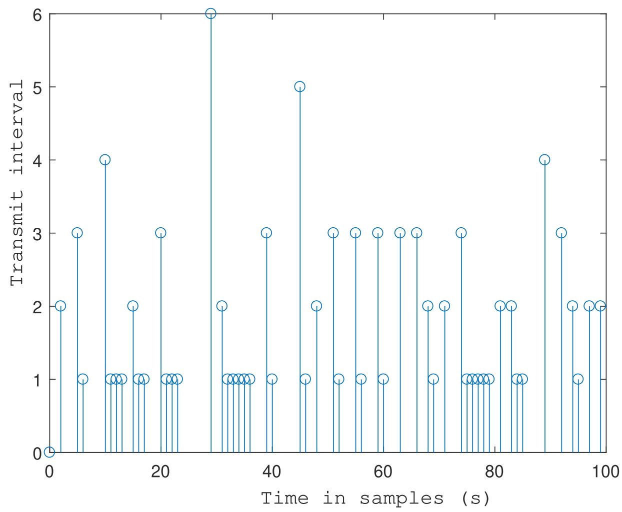

Fig. 9. The static event interval.

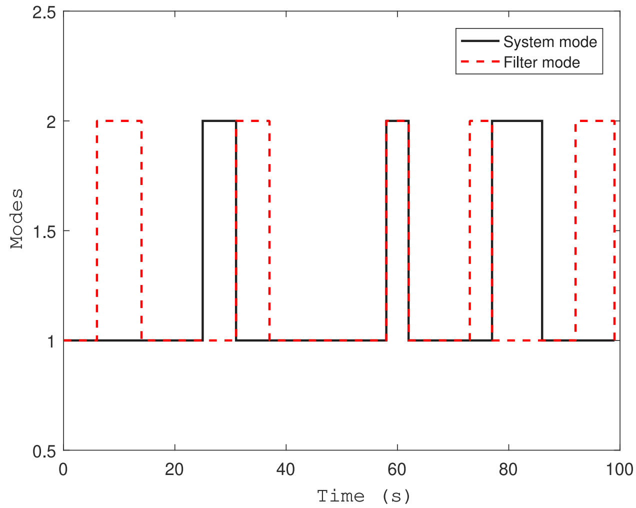

Fig. 10. The robot system and filter modes.

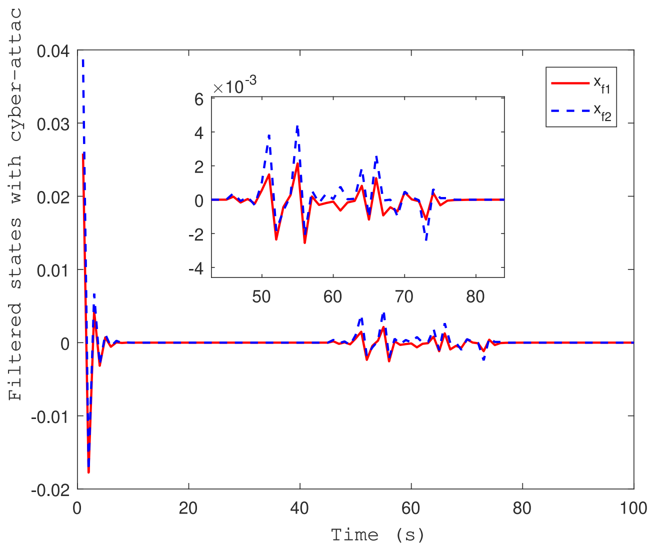

Fig. 11. Filtered states with cyber-attack (single-link robot arm example).

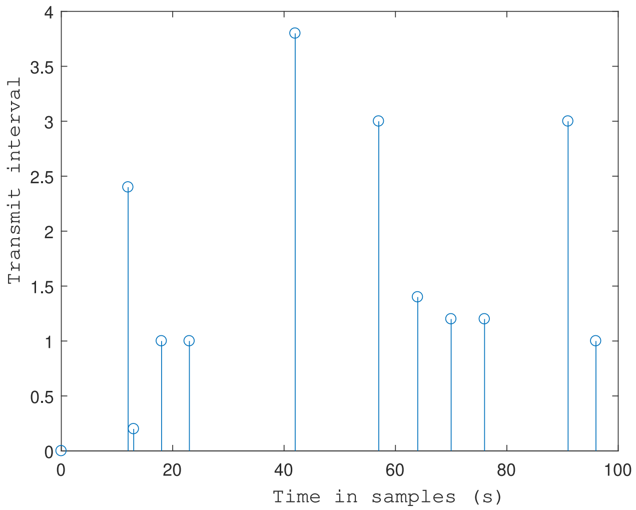

Fig. 12. The dynamic event interval (single-link robot arm example).

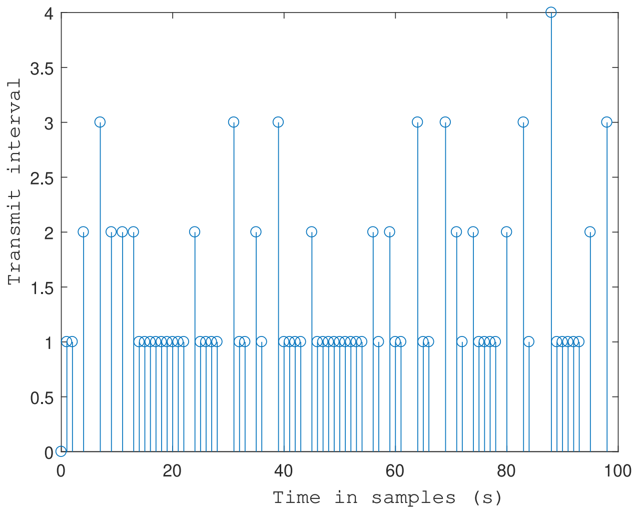

Fig. 13. The static event interval (single-link robot arm example).

results belong to theoretical numerical simulations, it provide a theoretical basis for other practical filtering engineering systems (such as circuit systems, mobile robot systems [40,41]).

5. Conclusion and future work

Asynchronous filtering problems are investigated for MJS with time-delay and external disturbances when nonlinear cyber-attacks occurred to the transmission processing. The dynamic event-triggered generator is constructed to judge and execute the transmission of measurement output state to save more network resources. Then the nonlinear cyber-attacks are analyzed during the data transmission process. According to the established asynchronous filter, the filtering error system dynamics are augmented and the overall filtering framework is presented. Next, the system stochastic stability is synthesized and by applying Lyapunov function as well as low-conservative time-delay lemma, stability conditions are derived. Subsequently, the asynchronous filter parameter expression are derived. Finally, two simulations are provided to show the proposed method can deal with cyber nonlinearities and effectively reduce the signal transmission, hence reduce the network burden.

In the future work, some novel filter design methods for nonlinear systems over sensor networks will be studied, such as extended Kalman approach [42] and set-membership approach [43].

Declaration of competing interest

The authors declare that they have no known competing financial interests or personal relationships that could have appeared to influence the work reported in this paper.

Acknowledgements

This work was supported in part by the National Natural Science Foundation of China under Grants U22A20101 and 62173051, in part by the Chongqing Technology Innovation and Application Development Special Key Project under Grants CSTB2022TIAD-CUX0015 and CSTB2022TIAD-KPX0162, and in part by graduate research and innovation foundation of Chongqing, China under Grant CYB22066.

References

[1] M. Li, M. Liu, Y. Zhang, H. Zhang, Asynchronous adaptive fault tolerant sliding mode control for T-S fuzzy singular Markovian jump systems with uncertain transition rates, IEEE Trans. Cybern. 52 (1) (2022) 544–555.

[2] Y. Tian, Z. Wang, Robust H-infinity filtering for singular Markovian jump systems via decoupling and substitution principles, Internat. J. Robust Nonlinear Control 31 (8) (2021) 3179–3197.

[3] G. Wang, L. Xu, Stability and stabilization for singularly perturbed systems with Markovian jumps, Internat. J. Robust Nonlinear Control 30 (12) (2020) 4690–4707.

[4] T. Zhang, Y. Wang, Z. Wei, MCL-STGAT: Taxi demand forecasting using spatio-temporal graph attention network with Markov cluster algorithm, Int. J. Innovative Comput. Inf. Control 19 (4) (2023) 1251–1264.

[5] G. Cheng, H. Liu, Asynchronous finite-time H_∞ filtering for linear neutral semi-Markovian jumping systems under hybrid cyber attacks, J. Franklin Inst. B 360 (3) (2023) 1495–1522.

[6] Y. Zhang, P. Shi, R.K. Agarwal, Y. Shi, Event-based dissipative analysis for discrete time-delay singular jump neural networks, IEEE Trans. Neural Netw. Learn. Syst. 31 (4) (2020) 1232–1241.

[7] H. Zhang, Z. Chen, N. Zhao, B. Xing, M. Kalidass, Adaptive neural dissipative control for Markovian jump cyber–physical systems against sensor and actuator attacks, J. Franklin Inst. B 360 (2023) 7676–7698.

[8] H. Zhang, X. He, L.I. Minchala, P. Shi, Dissipative output feedback control for semi-Markovian jump systems under hybrid cyber-attacks, J. Franklin Inst. B 358 (5) (2021) 2683–2702.

[9] Z. Cao, Y. Niu, H.K. Lam, J. Zhao, Sliding mode control of Markovian jump fuzzy systems: A dynamic event-triggered method, IEEE Trans. Fuzzy Syst. 29 (10) (2021) 2902–2915.

[10] Q. Chen, D. Tong, W. Zhou, Finite-time stochastic boundedness for Markovian jumping systems via the sliding mode control, J. Franklin Inst. B 359 (10) (2022) 4678–4698.

[11] C. Wang, R. Li, X. Su, P. Shi, Output feedback sliding mode control of Markovian jump systems and its application to switched boost converter, IEEE Trans. Circuits Syst. I. Regul. Pap. 68 (12) (2021) 5134–5144.

[12] C. Gong, G. Zhu, P. Shi, Adaptive event-triggered and double-quantized consensus of leader-follower multiagent systems with semi-Markovian jump parameters, IEEE Trans. Syst. Man Cybern. A 51 (9) (2021) 5867–5879.

[13] Z. Cao, Y. Niu, J. Song, Finite-time sliding-mode control of Markovian jump cyber–physical systems against randomly occurring injection attacks, IEEE Trans. Automat. Control 65 (3) (2020) 1264–1271.

[14] J. Liu, Y. Gu, X. Xie, D. Yue, J.H. Park, Hybrid-driven-based H_∞ control for networked cascade control systems with actuator saturations and stochastic cyber attacks, IEEE Trans. Syst. Man Cybern. A 49 (12) (2019) 2452–2463.

[15] L. Zha, R. Liao, J. Liu, X. Xie, J. Cao, L. Xiong, Finite-time adaptive event-triggered asynchronous state estimation for Markov jump systems with cyber-attacks, Internat. J. Robust Nonlinear Control 32 (2) (2022) 583–599.

[16] J. Liu, Y. Gu, J. Cao, S. Fei, Distributed event-triggeredH_∞ filtering over sensor networks with sensor saturations and cyber-attacks, ISA Trans. (2018) http://dx.doi.org/10.1016/j.isatra.2018.07.018.

[17] J. Wu, C. Peng, J. Zhang, B. Zhang, Event-triggered finite-time H_∞ filtering for networked systems under deception attacks, J. Franklin Inst. B 357 (6) (2020) 3792–3808, http://dx.doi.org/10.1016/j.jfranklin.2019.09.002.

[18] W. Xie, Y. Zeng, K. Shi, X. Wang, Q. Fu, Hybrid event-triggered filtering for nonlinear Markov jump systems with stochastic cyber-attacks, IEEE Access 9 (2021) 248–258.

[19] Y. Wang, P. He, P. Shi, H. Zhang, Fault detection for system with model uncertainties and disturbances via coprime factorization and gap metric, IEEE Trans. Cybern. 52 (8) (2022) 7765–7775.

[20] R. Ragul, G. Sangeetha, K. Mathiyalagan, H. Zhang, Exponential stability results for stochastic semi-linear systems with levy noise, Int. J. Innovative Comput. Inf. Control 18 (6) (2022) 1929–1940.

[21] H. Li, J. Xu, Y. Yang, X. Zhang, Novel switchable filtering circuit with function reconfigurability between SPQT filtering switch and four-way filtering power divider, IEEE Trans. Microw. Theory Tech. 68 (3) (2020) 867–876.

[22] R.N. Beres, X. Wang, F. Blaabjerg, M. Liserre, C.L. Bak, Optimal design of high-order passive-damped filters for grid-connected applications, IEEE Trans. Power Electron. 31 (3) (2016) 2083–2098.

[23] J. Kim, S.S. Vaddi, P.K. Menon, E.J. Ohlmeyer, Comparison between nonlinear filtering techniques for spiraling ballistic missile state estimation, IEEE Trans. Aerosp. Electron. Syst. 48 (1) (2012) 313–328.

[24] G. Deng, An entropy interpretation of the logarithmic image processing model with application to contrast enhancement, IEEE Trans. Image Process. 18 (5) (2009) 1135–1140.

[25] D. Schwingshackl, G. Kubin, Polyphase representation of multirate nonlinear filters and its applications, IEEE Trans. Signal Process. 55 (5) (2007) 2145–2157.

[26] A.P.C. Goncalves, A.R. Fioravanti, J.C. Geromel, $\mathcal{H}_\infty$ filtering of discrete-time Markov jump linear systems through linear matrix inequalities, IEEE Trans. Automat. Control 54 (6) (2009) 1347–1351.

[27] G. Zhuang, S. Su, J. Xia, W. Sun, HMM-based asynchronous H_∞ filtering for fuzzy singular Markovian switching systems with retarded time-varying delays, IEEE Trans. Cybern. 51 (3) (2021) 1189–1203.

[28] F. Lin, J. Zhang, X. Jia, X. Zhou, Adaptive event-triggering distributed filter of positive Markovian jump systems based on disturbance observer, J. Franklin Inst. B 360 (4) (2023) 2507–2537.

[29] N. Zhao, X. Zhao, M. Chen, G. Zong, H. Zhang, Resilient distributed event-triggered platooning control of connected vehicles under denial-of-service attacks, IEEE Trans. Intell. Transp. Syst. 24 (6) (2023) 6191–6202.

[30] B. Jiang, Y. Shen, H. Dong, F. Han, G. Li, Dynamic event-based recursive filtering for networked systems under the encoding-decoding mechanism, J. Franklin Inst. B 359 (12) (2022) 6503–6522.

[31] H. Zhang, N. Zhao, S. Wang, R.K. Agarwal, Improved event-triggered dynamic output feedback control for networked T-S fuzzy systems with actuator failure and deception attacks, IEEE Trans. Cybern. (2023) http://dx.doi.org/10.1109/TCYB.2023.3264820.

[32] S. Zhang, J. Zhang, G. Zheng, Hybrid gain performance-based random event-triggered filter of positive semi-Markovian jump systems with intermittent sensor faults, Internat. J. Robust Nonlinear Control 32 (3) (2022) 1425–1452.

[33] X. Liu, X. Su, P. Shi, C. Shen, Y. Peng, Event-triggered sliding mode control of nonlinear dynamics systems, Automatica 112 (2020) 108738.

[34] H. Khalil, Nonlinear Systems, Prentice-Hall, NJ, 1996.

[35] Z. Wu, P. Shi, H. Su, J. Chu, Asynchronous l_2-l_∞ filtering for discrete-time stochastic Markov jump systems with randomly occurred sensor nonlinearity, Automatica 50 (2014) 180–186.

[36] G. Kreisselmeier, Stabilization of linear systems in the presence of output measurement saturation, Syst. Control Lett. 29 (1996) 27–30.

[37] S.J. Kim, I.J. Ha, A state-space approach to analysis of almost periodic nonlinear systems with sector nonlinearities, IEEE Trans. Automat. Control 44 (1) (1999) 66–70.

[38] J. Lam, H. Gao, S. Xu, C. Wang, H_∞ and L_2/L_∞ infinity model reduction for system input with sector nonlinearities, J. Optim. Theory Appl. 125 (1) (2005) 137–155.

[39] Z. Wu, P. Shi, Z. Shu, H. Su, R. Lu, Passivity-based asynchronous control for Markovian jump systems, IEEE Trans. Automat. Control 62 (4) (2017) 2020–2025.

[40] H. Zhang, X. Zheng, H. Yan, C. Peng, Z. Wang, Q. Chen, Codesign of event-eriggered and distributed H_∞ filtering for active semi-vehicle suspension systems, IEEE/ASME Trans. Mechatronics 22 (2) (2017) 1047–1058.

[41] T. Zhang, F. Deng, P. Shi, Event-triggered H_∞ filtering for nonlinear discrete-time stochastic systems with application to vehicle roll stability control, Internat. J. Robust Nonlinear Control 30 (18) (2020) 8430–8448.

[42] A. Barrau, S. Bonnabel, Extended Kalman filtering with nonlinear equality constraints: A geometric approach, IEEE Trans. Automat. Control 65 (6) (2020) 2325–2338.

[43] D. Ding, Z. Wang, Q. Han, A set-membership approach to event-triggered filtering for general nonlinear systems over sensor networks, IEEE Trans. Automat. Control 65 (4) (2020) 1792–1799.